



Comparative analysis of the propagation conditions of millimeter radio waves at the NIRFI NNSU "Karadag" site (southeastern Crimea), the "Suffa" plateau (southern Uzbekistan) and three IAA RAS test sites located in different climatic zones of the Russian Federation

*I. T. Bubukin¹, M. I. Agafonov¹, I. V. Rakut^{1,2,3}, A. L. Pankratov^{1,2,3},
A. A. Yablokov^{2,3}, T. U. Gorbunova⁴, P. V. Gorbunov⁴*

¹*Научно-исследовательский радиофизический институт ННГУ им. Н.И. Лобачевского, 603950, г. Нижний Новгород, ул. Большая Печерская, 25/12а*

E-mail: bubn10@mail.ru

²*Институт физики микроструктур РАН, филиал ФИЦ ИПФ РАН, 603950, г. Нижний Новгород, ГСП-105*

E-mail: alp@ipmr.ru

³*Нижегородский государственный технический университет им. Р.Е. Алексеева, г. Нижний Новгород, ул. Минина, 24*

⁴*ФГБУН «Институт морских биологических исследований им. А.А. Ковалевского РАН», 299011, г. Севастополь, проспект Нахимова, 2*

E-mail: karadag_station@mail.ru

Бубукин И.Т.

ст.: +79870831535

E-mail: bubn10@mail.ru

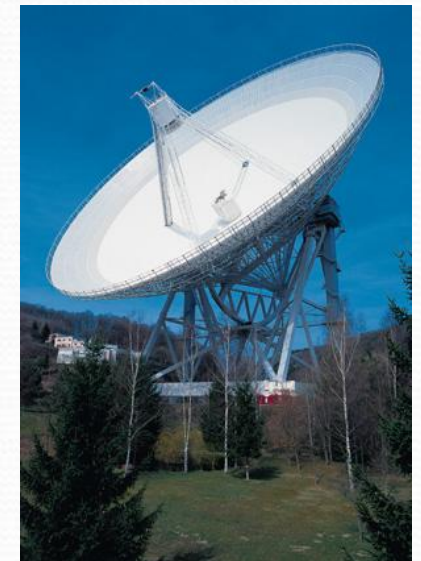
Selection criteria

The criterion for choosing the location of a radio astronomy observatory operating in the millimeter wave range is a consistently good and well-predictable atmospheric transparency in the millimeter wave range.

Chahnantor Plateau (Chile) Atacama Large Millimeter Array (ALMA)



Vegetation as an indicator of moisture content



Koluch-Kul / Shorbulak — 54 km



Shorbulak Plateau (Eastern Pamir)



The first mm studies in the Eastern Pamir during the expedition of the Nizhny Novgorod Radiophysical Institute (June-Nov. 1962). All the photos are kindly provided by L.V. Lubyako, participated in these measurements.

Surroundings nearby a) Koluch-Kul Cosmic Ray Station of the Lebedev Physical Institute of the RAS,
b) Shorbulak observatory. Both photos are kindly provided by A.S. Borisov, a head of the Pamir Cosmic Ray Station.

Alexander V. Lapinov, Svetlana A. Lapinova, Leonid Yu. Petrov, Daniel Ferrusca, "On the benefits of the Eastern Pamirs for sub-mm astronomy," Proc. SPIE 11453, Millimeter, Submillimeter, and Far-Infrared Detectors and Instrumentation for Astronomy X, 114532O (13 December 2020); doi: 10.1117/12.2560250

Suffa Plateau : RT-70 (southern Uzbekistan)



Географическое расположение и местоположение плато Суффа на отрогах Туркестанского хребта. Долгота $65^{\circ} 26'$, широта $39^{\circ} 37'$. Высота над уровнем моря 2500 метров. Максимальный угол закрытия горизонта 9° .

Панорама строительства радиообсерватории 1999г.

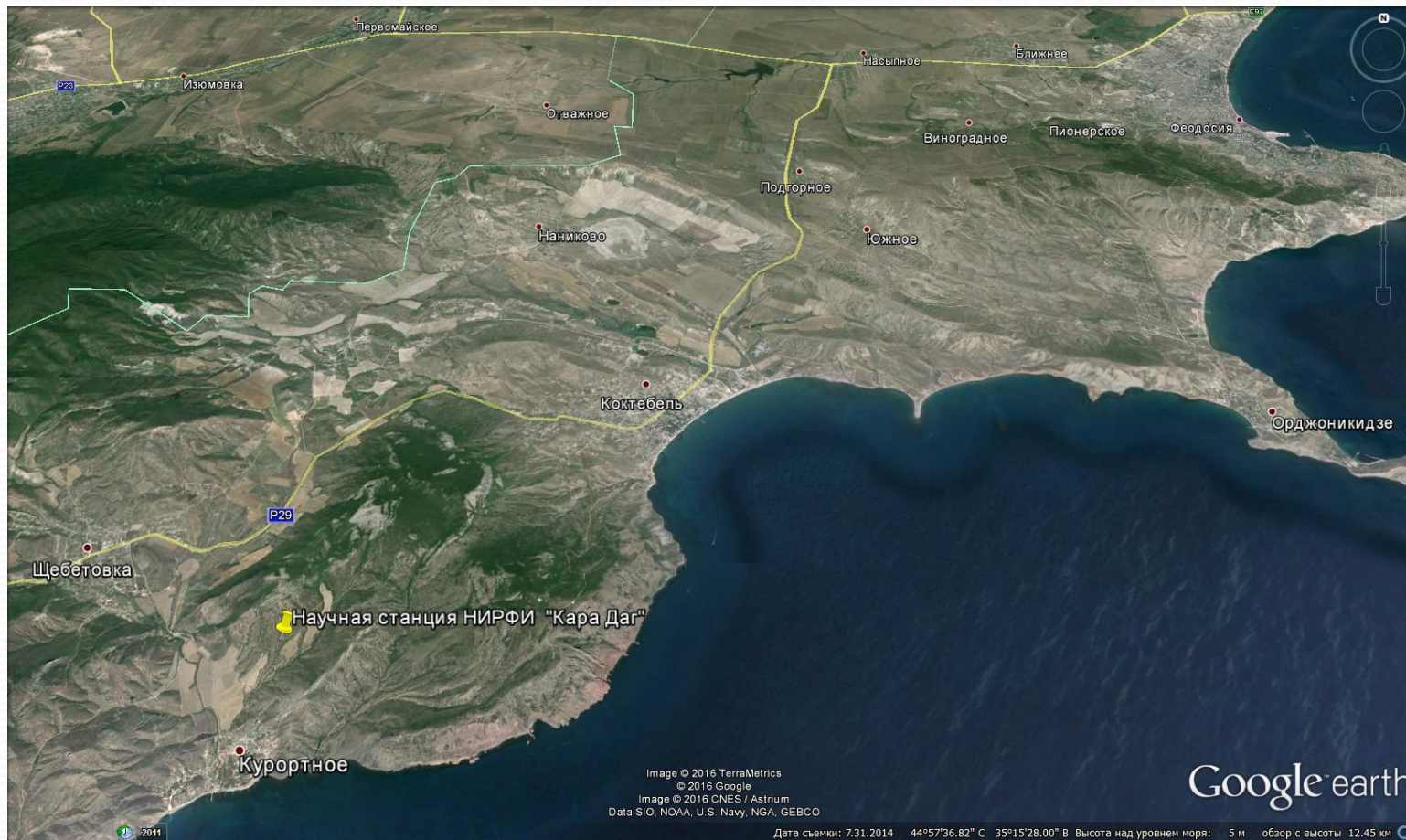


Закладка камня на месте строительства радиообсерватории.
Рашидов Ш.Р., Котельников В.А., май 1981 год.



Макет комплекса радиообсерватории на плато Суффа.
1. Радиотелескоп RT-70
2. Монтажно-испытательный корпус
3. Надземный переход
4. Блок дежурных наблюдателей с антенной космической связи
5. Главное здание с вычислительным центром и лабораторией мониторинга атмосферы

Results of measurements of atmospheric transparency parameters and their relation to climatic features at the location of the Karadag landfill.





Щетовка

P29

Научная станция НИРФИ "Кара Даг"

Курортное

© 2016 Google
Image © 2016 CNES / Astrium

Google earth

2008

Дата съемки: 6.17.2014 44°55'10.14" С 35°11'20.24" В Высота над уровнем моря: 36 м обзор с высоты 2.69 км

External calibration of antennas on the "Artificial Moon" test site "Karadag"



V. S. Troitsky at the radio telescope after the observation session. Crimea, Kara-Dag. 1965

$$d(\theta) = k \cdot T_{\text{Я}}(\theta) + A$$

Calibration step = disk-brightness
temperature of the sky behind the disk

"Artificial Moon" – a black-body disk raised on a rocky ledge of the "Balaly-Kaya" ridge

Far antenna area

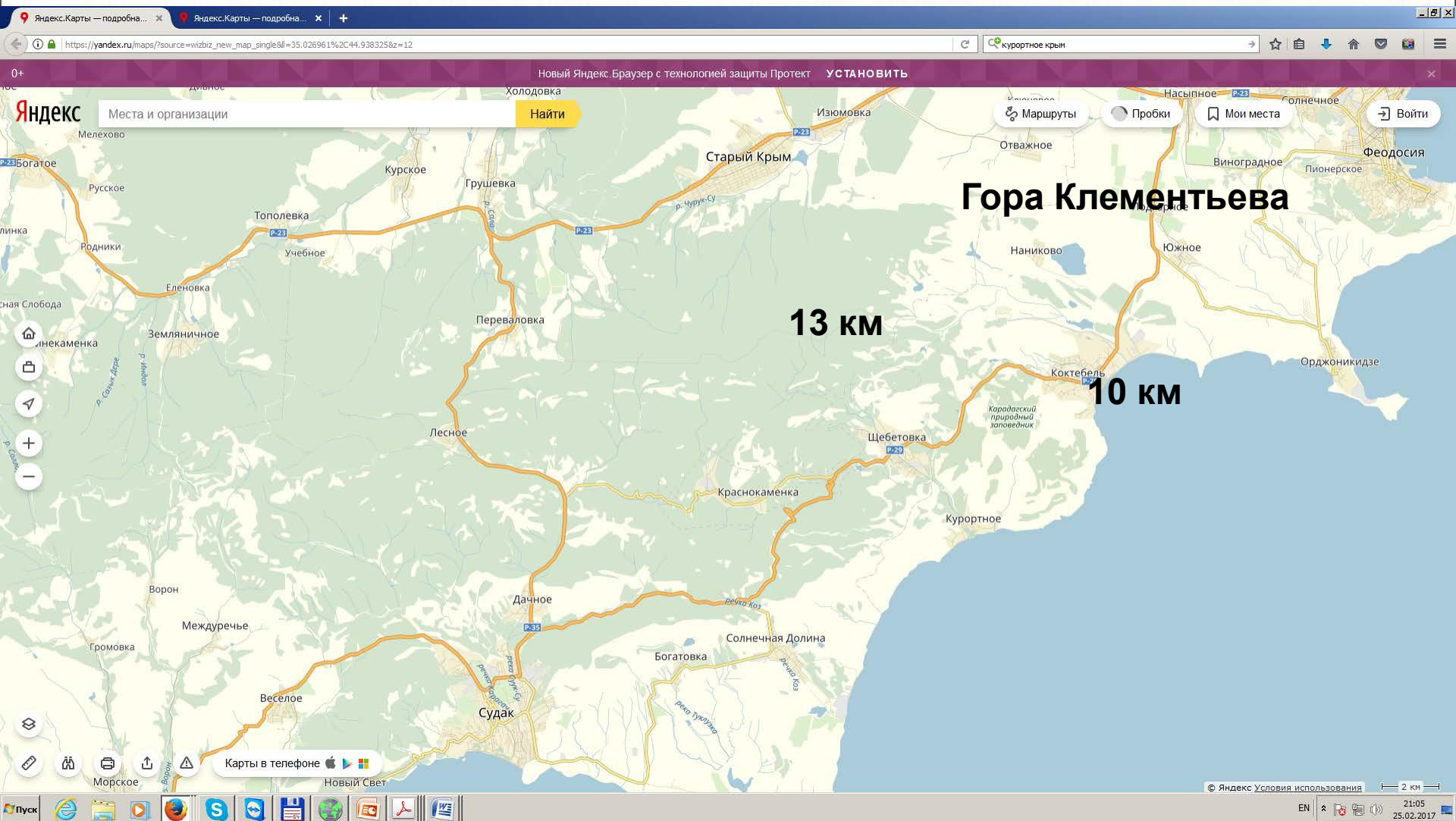
$$R > \frac{D^2}{\lambda}$$



Radio telescopes on the upper site. On the mountain – "Artificial Moon". Crimea, Kara-Dag. 80-ies.



Choosing the location of the optical telescope before the World War II



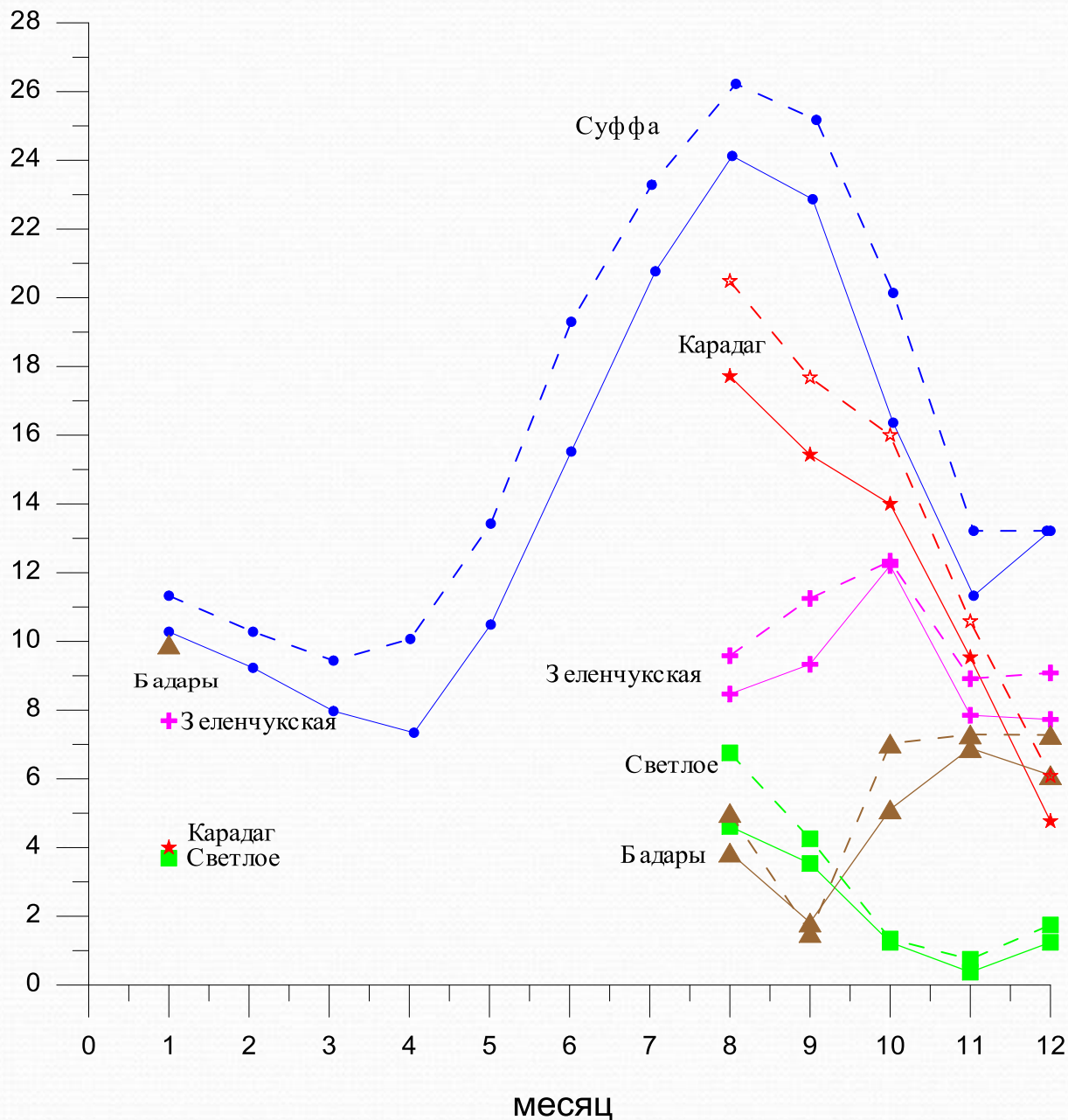
Comparative assessment of weather conditions based on meteorological data for the Karadag landfill, the Suffa plateau and three landfills of the IAA RAS

The methodological basis for the comparison at the first stage was the approach used in the selection of the Suffa plateau.

The main factors affecting the propagation of MMW in the atmosphere are the absorption in atmospheric gases - oxygen and water vapor, as well as the droplet fraction of clouds. Therefore, as a rule, the minimum atmospheric absorption of MICEX is observed in clear, cloudless weather. Consider two important parameters for polygons: Parameter 1 – the number of clear days and nights, Parameter 2 - the surface temperature, on which the phase states of atmospheric moisture depend.

Parameter 1. Clear days and clear nights. The number of clear days per year was one of the main factors in choosing the "Suffa" plateau. Weather conditions were considered favorable for radio astronomy measurements in the millimeter range with a cloud cover of less than 2.5 points (the percentage of cloud cover in the sky is less than 25%). Automatic weather stations at the Karadag and IAA RAS test sites do not register the state of clouds, so we used data from the nearest weather stations of Roshydromet, which have weather archives on the resource "rp5.ru". For the "Karadag" landfill, this is a weather station in the village Kurortnoye (No. 33957), at a distance of 3 km from the landfill, for the landfill "Svetloye" - a weather station in the village of Sosnovo (No. 22891), at a distance of 25 km, for the landfill "Zelenchukskaya" - a weather station in the village of Zelenchukskaya (No. 37112), at a distance of 5 km and for the landfill "Badary" - a weather station in the village of Kyren (No. 30806), at a distance of 10 km.

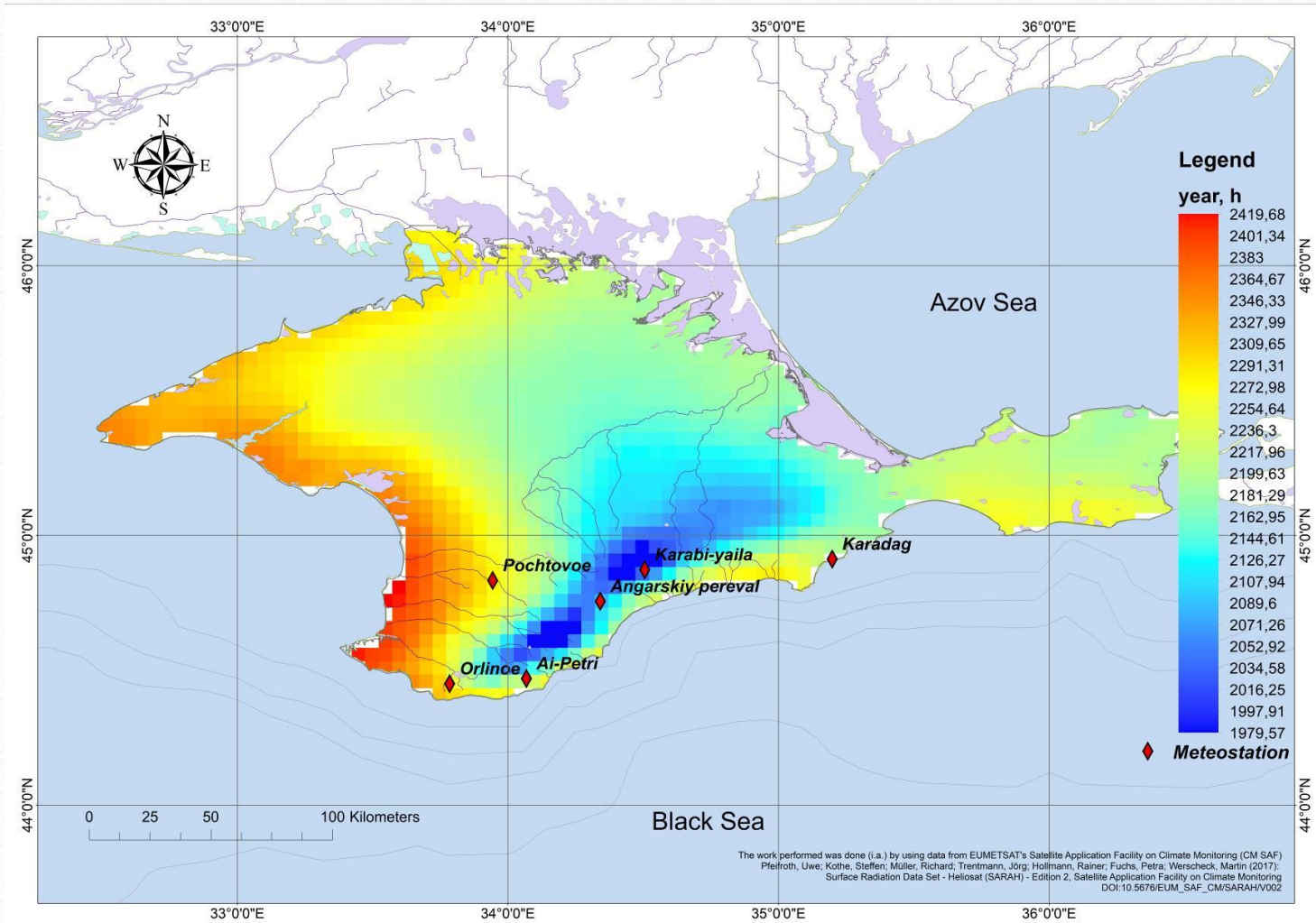
КОЛИЧЕСТВО СУТОК



The average data on time intervals in days with cloud cover of less than 2.5 points are represented by solid lines for months for 1981-1991 for the "Suffa" plateau (blue dots), as well as for other polygons for months from August 2019 to January 2020. For the time intervals when the MMV propagation conditions were measured: "Karadag" (red stars), "Svetloe" (green squares), "Zelenchukskaya" (purple crosses), "Badary" (brown triangles). Dotted line – clear nights.

In the summer-autumn period, the proportion of clear weather for Karadag significantly exceeds this parameter for the IAA RAS polygons and is comparable to the data for Suffa.

**The duration of the sunshine on the territory of the Crimean Peninsula, h.
The map is based on the data of the reanalysis performed on the materials
of the European Organization of Satellite Meteorology**



The greatest duration of the solar radiance is observed in the area of the Yevpatoria space communication point, located in the western Crimea. However, the shorter duration of sunshine in the Karadag region (by about 8%) is associated with the mountainous nature of the terrain in the south-eastern Crimea, which leads to a shorter duration of the sunny day.

The nature of vegetation in the area of the Yevpatoria space communication point

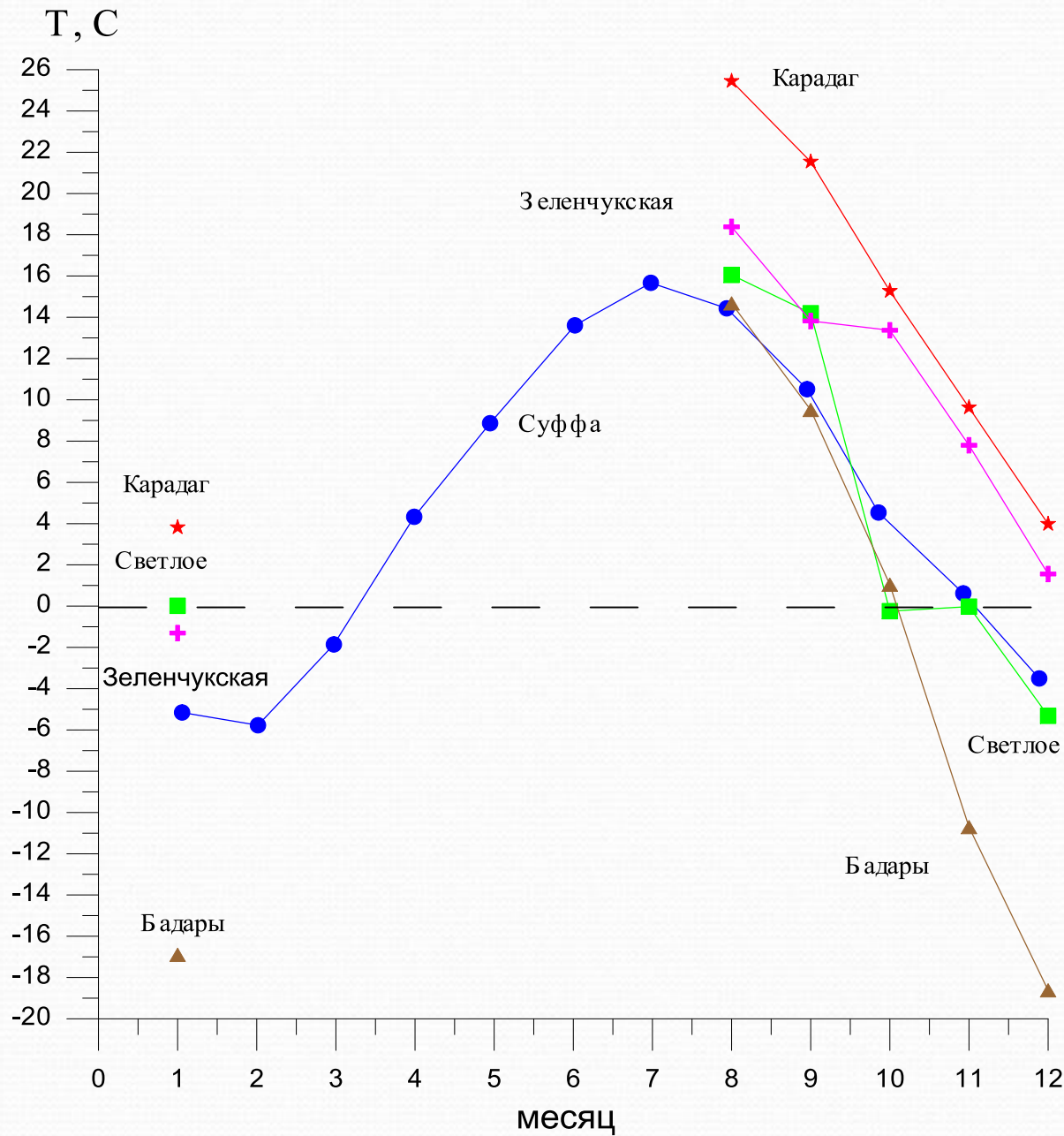


General view from Vitino village



The flat nature of the terrain in the area of Yevpatoria contributes to the free spread of moist sea air deep into the land. Unfortunately, at the moment there are no data for measuring the integral moisture content of the atmosphere in the western Crimea. However, the surface values of absolute humidity and the nature of vegetation indicate a lower moisture content in the area of the Karadag landfill than in Yevpatoria. The territories around the sites of the Yevpatoria space communication station are actively used for growing agricultural crops, while only grapes grow in the area of the Karadag landfill.

70-m antenna P-2500 (RT-70)



Average monthly surface temperatures with clouds less than 2.5 points for 1981-1991: for "Suffa" - blue dots, for other polygons from August 2019 to January 2020: "Karadag" – red stars, "Svetloe" – green squares, "Zelenchukskaya" – purple crosses, "Badary" - brown triangles. The temperature data for the polygons are taken from their own weather stations. It can be seen that the highest temperatures are observed in Karadag, the lowest - in Badary and Suffa. During the period under review, all average monthly temperatures on Karadag are positive. In the autumn-winter period, negative temperatures appear on the Suffa and all the landfills of the IAA RAS. The lowest temperatures are observed in Badary due to the sharply continental climate in central Siberia. They also appear on the high-altitude plateau of Suffa (2335 m), despite the hot climate of southern Uzbekistan. Even in summer, temperatures for Suffa do not exceed 16°C.

Specialized radiometric system for atmospheric diagnostics.

$$T_{\mathcal{R}}(\theta) = T_{cp} \left(1 - e^{-\frac{\tau}{\cos\theta}} \right) + 2.73 \cdot e^{-\frac{\tau}{\cos\theta}} \quad Q = \int_0^{\infty} \rho_{H_2O}(h) dh \quad \alpha_{H_2O}(h) = \varphi_{H_2O}(h) \rho_{H_2O}(h) \quad \tau_{H_2O} = \int_0^{\infty} \alpha_{H_2O}(h) dh = \int_0^{\infty} \varphi_{H_2O}(h) \rho_{H_2O}(h) dh \cong \bar{\varphi}_{H_2O}(\lambda) Q$$

$$\tau(v_{\alpha}), \alpha = 1, 2 \quad \tau(v_{\alpha}) = \tau_{o_2}(v_{\alpha}) + \varphi_{H_2O}(v_{\alpha}) \cdot Q + \psi_w(v_{\alpha}) \cdot W \quad \nu_1 \approx 60 - 90 \text{ ГГц} \quad \nu_2 \approx 30 \div 40 \text{ ГГц} \quad \nu_3 \approx 56.7 \text{ ГГц}$$

Typically, atmospheric radiation is used in the transparency window at a wavelength of 0.8 cm, the absorption lines of oxygen and water vapor at wavelengths of 0.5 cm and 1.35 cm.

The spectral line H₂O 1.35 cm is weak enough to measure small amounts of water vapor Q in the atmosphere. In this case, it is preferable to use a strong H₂O absorption line 183 GHz (1.64 mm), or rather its long-wave slope in the range of 70-110 GHz, (~3 mm) in the transparency window between the strong atmospheric oxygen absorption lines of 60 GHz and 120 GHz.

Measurements of the integral moisture content of the atmosphere at the IAA RAS landfills by the tropospheric signal delay in precision positioning systems.

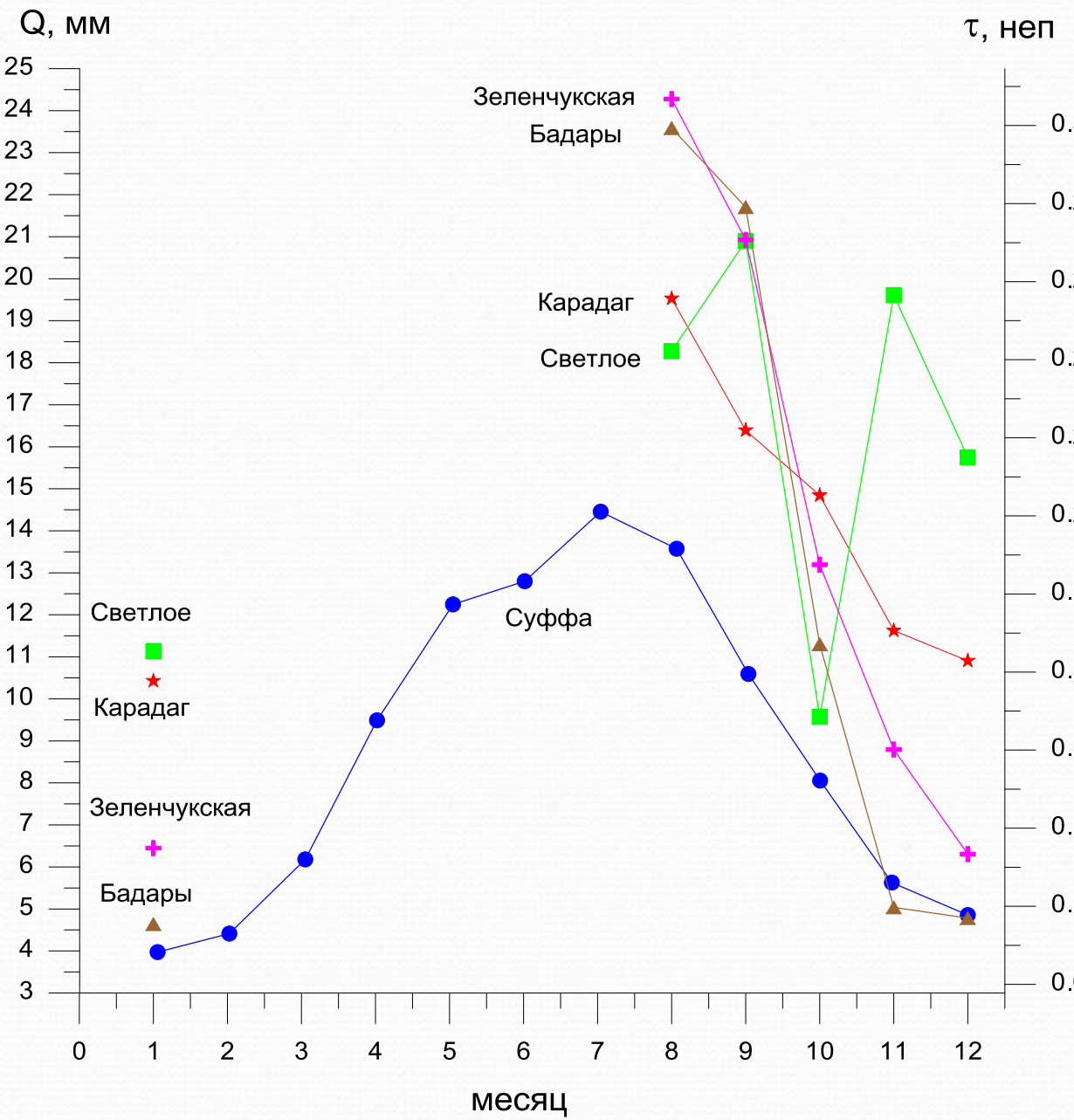
For a comparative analysis of the conditions for the propagation of MMW in different places, it is desirable to have for them the results of simultaneous measurements of the integral moisture content of the atmosphere. Unfortunately, the results of atmospheric absorption measurements for the IAA RAS polygons have not been published. Therefore, for a comparative analysis of the conditions for the propagation of MMV, we used publicly available data from measurements of the tropospheric signal delay for the IPA RAS polygons .

$$\text{Tropospheric delay the signal } \lambda \geq 1 \text{ MM} \quad \Delta l_{\phi} [cM] = \int_0^{H_A} (n-1) dl = \sec \theta \left(0.2279 \cdot P_0 [zPa] + 0.109 \cdot Q [z/cM^2] + \frac{1730}{T_Q [K]} Q [z/cM^2] + 0.145 \cdot W [Kz/M^2] \right)$$

n – refractive index of air, H_A – atmospheric altitude, P_0 – ground pressure, T_Q – the average temperature of the atmosphere weighted by absolute humidity, W – integral water content of clouds.

Based on the data on the total tropospheric zenith path delay (cm) from and the hydrostatic component (dry troposphere path delay, cm) described by the first component, in clear weather conditions, the integral moisture content is determined by the ratio:

$$Q [z/cM^2] = (\Delta l_{ZPD} - \Delta l_{DPD}) / \left(0.109 + \frac{1730}{T_Q [K]} \right)$$



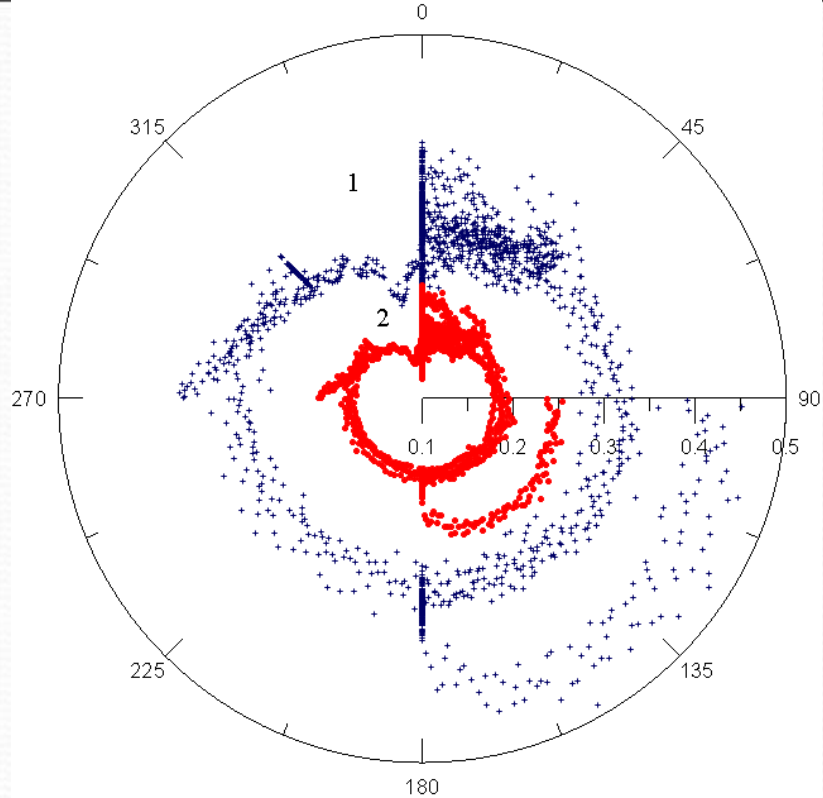
Graphs of measurements of the integral moisture content with clouds less than 2.5 points (left scale) for 1981-1991. For "Suffa" - blue dots, for other polygons from August 2019 to January 2020: "Karadag" - red stars, "Svetloe" - green squares, "Zelenchukskaya" - magenta crosses, "Badary" - brown triangles. The right scale shows the atmospheric absorption measurements in the range of 3 mm for the Karadag sites and illustrates the atmospheric absorption values corresponding to the integral moisture content (left scale) for the Suffa and the IAA RAS sites, if such measurements were carried out there in the range of 3 mm. The decline in the integral moisture content in winter for the Suffa and landfills of the IAA RAS is associated with the transition to negative temperatures

The graphs show that the average monthly water vapor content for the Karadag landfill is 5-7 mm more deposited moisture than for the Suffa. When selecting the Suffa, two parameters were used as the criterion, the number of clear days and the water vapor content. A comparison of these parameters allows us to conclude that the number of clear days at the Suffa and Karadag landfills does not differ significantly, and the water vapor content at Karadag is 20-30% higher than at Suffa. However, it should be noted that the height of Karadag above sea level (105 m), which is 22 times less than that of Suffa (2335 m). Thus, the use of high mountains in this case, within the framework of the standard approach for choosing the installation locations of the MMV band antennas, gives a weak effect. At the same time, a comparison of the data on the surface temperature and the integral moisture content for Suffa and Karadag shows that at the same temperatures, the integral moisture content is approximately equal. For example, the surface temperatures in August for Suffa are approximately equal to the October temperature for Karadag, and the integral moisture content for Suffa in August is approximately equal to the integral moisture content for Karadag in October. Thus, this example shows that the surface temperature is one of the main factors influencing the integral moisture content, including in the highlands. The average summer temperatures on the Suffa plateau due to the highlands are 14-16° C, although the Ferghana Valley is nearby with high summer temperatures. In winter, the surface temperatures for Suffa become negative in contrast to Karadag, and the main factor that leads to a decrease in the integral moisture content in winter for Suffa is freezing. At negative temperatures, water vapor in the atmosphere crystallizes, and the absorption in ice crystals is significantly less than in water vapor. This also confirms the fact that the main factor that determines the choice of location within the standard approach is low ground temperatures.

An alternative approach to the choice of installation sites for MMV antennas on the example of the "Karadag" site

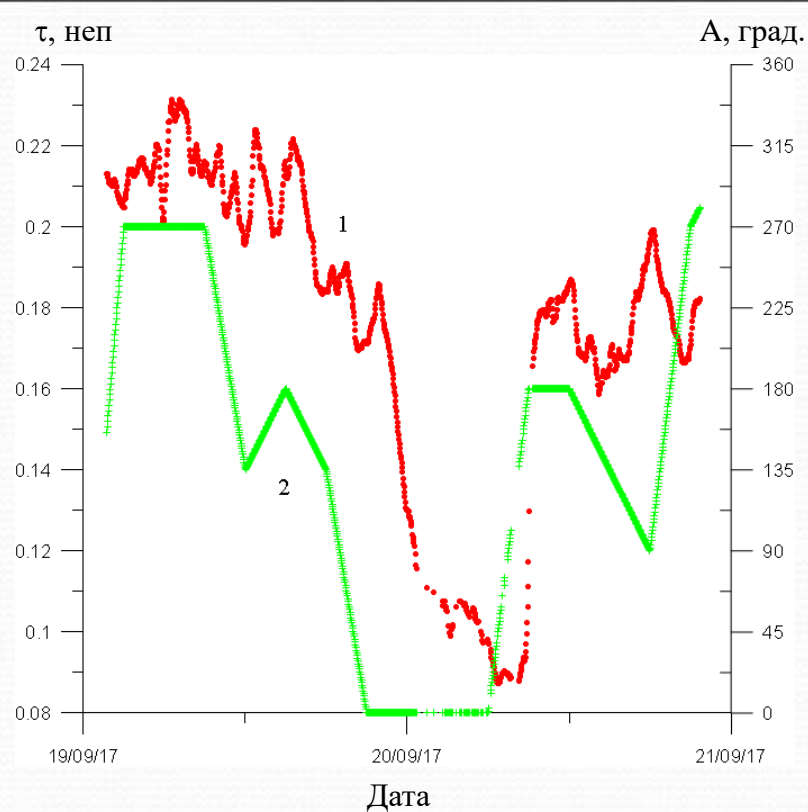
The Karadag mountain range is located on the sea coast and has a specific configuration with the formation of semi-enclosed areas, with a change in altitude and a set of mountain ranges, which are mainly located along the coast in several rows. This configuration creates a variety of climatic conditions. The Karadag landfill is located near the border of the reserve and is protected from the sea from the east by two ridges of mountains. The combination of features of atmospheric circulation over the Karadag massif, located on the border of the sea and land, causes significant amounts of solar radiation with relatively low clouds. On Karadag, the winds of the northern directions prevail, carrying dry cold air from the flat Crimea. During the year, their frequency exceeds 60% . During the incursions of cold air masses, which, passing over a low ridge, are relatively little heated adiabatically and "fall" down the leeward slope at a high speed under the influence of a pressure gradient and gravity, drying the atmosphere, a local boron wind is formed, which determines the high transparency of the atmosphere. The average climatic effective height of water vapor in the area of the Karadag landfill according to measurements at a wavelength of $1.35 \text{ cm} \cdot h = 1.9 \text{ km}$





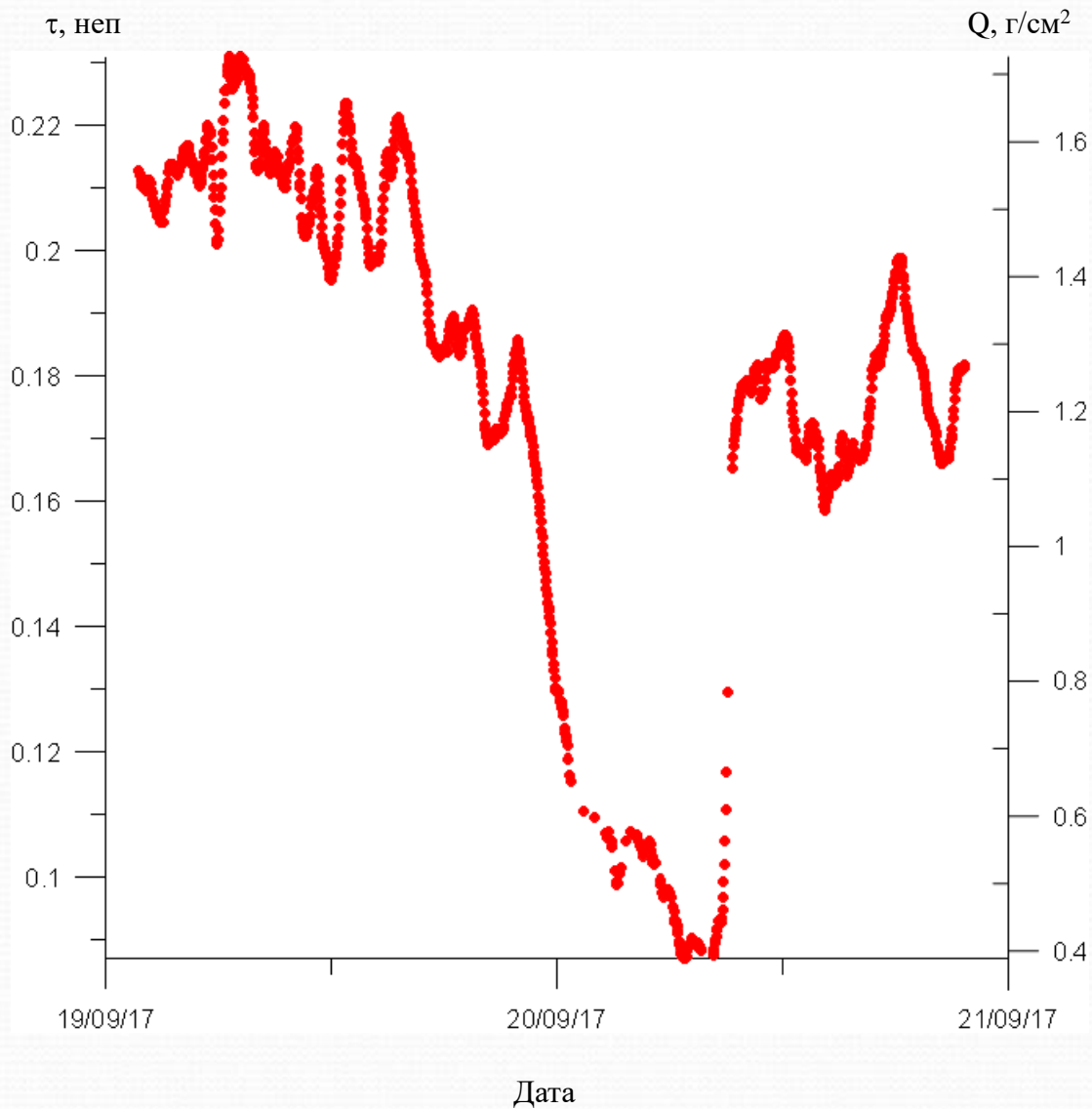
2017 г.

τ , неП



Plot of azimuthal dependence of atmospheric absorption in radiometric channels 3 mm (red, dots-2) and 2 mm (blue, crosses - 1). Atmospheric absorption is plotted along the radial axis, and the azimuthal axis shows the direction from which the wind blows A (deg.) - in the measurement area from July 29 to August 2, 2017. Zero degrees corresponds to the north direction. The average temperature of the atmosphere weighted by absolute humidity

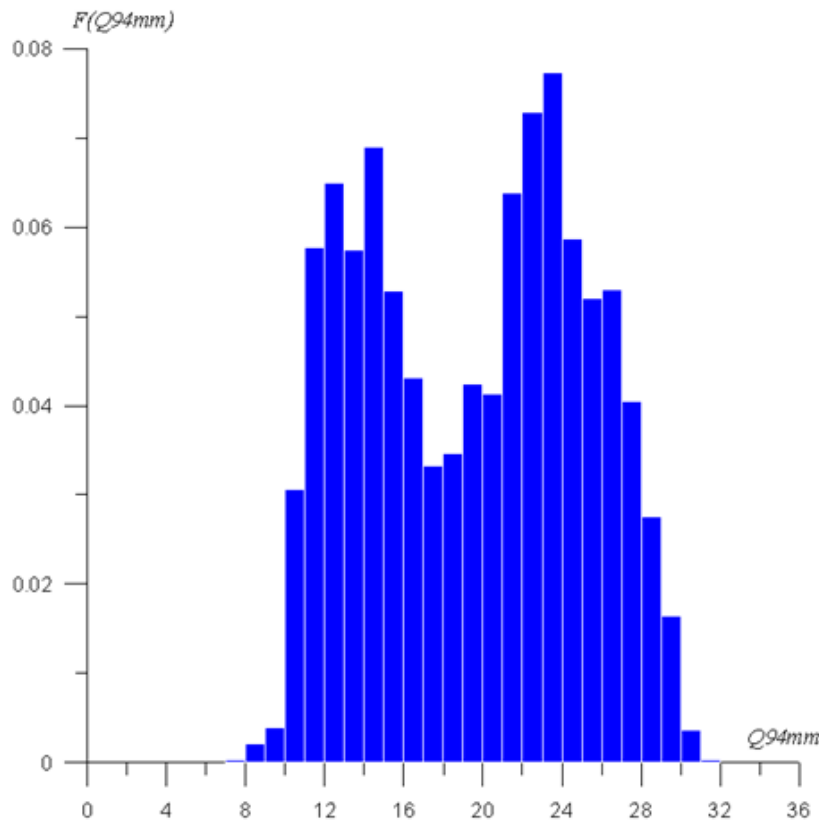
Graphs of atmospheric absorption measurements for the wavelength of 3 mm (red, dots-1) - left scale and the direction from which the wind blows A (green, crosses-2) - right scale from September 19 to 21, 2017 at the Karadag test site. Zero degrees corresponds to the north direction. Over a time interval of about 8 hours, there is a sharp decrease in absorption for a wavelength of 3 mm. When the wind direction changes to the north, the absorption decreases with a certain time delay.



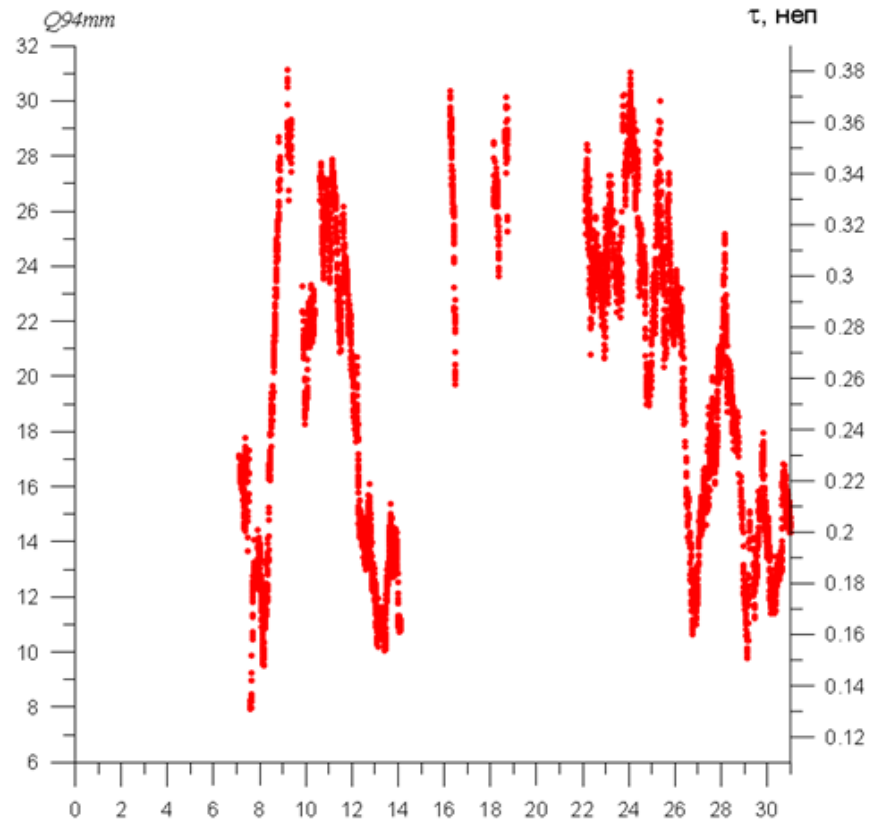
2017 г.

The values of atmospheric absorption-the left scale and the integral water vapor content Q-the right scale, measured by the radiometric method for absorption at a wavelength of 3 mm. Q is given in units of g/cm² used in meteorology. In mm of deposited moisture, 1 g / cm² corresponds to 10 mm. Q drops to 3-4 mm of deposited moisture, which is a good indicator, corresponding to the best values for high-altitude telescopes.

2019 г.



a)

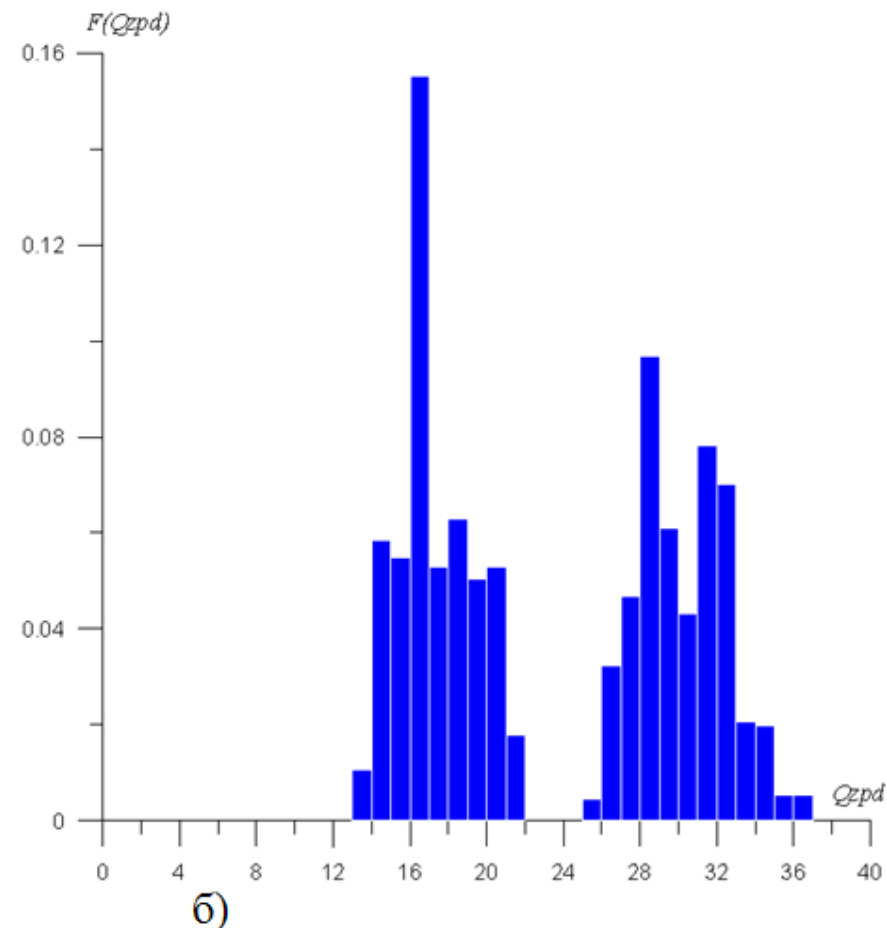
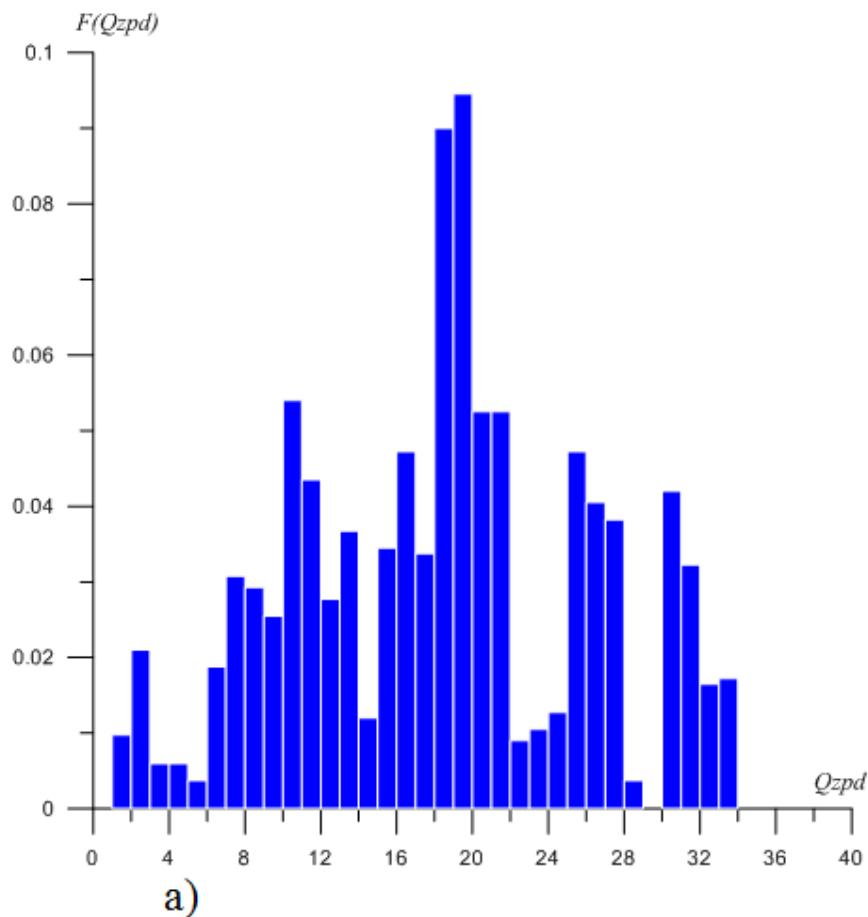


б)

a) A histogram of the measured values of the integral moisture content in the atmosphere in millimeters of deposited moisture for a wavelength of 3 mm at the Karadag test site with two maxima for August 2019. The histogram is constructed from 5655 measurements; b) the time dependence (horizontal axis in fractions of a day from the beginning of the month) of the values of the integral moisture content in the atmosphere in millimeters of deposited moisture at the Karadag test site for August 2019.

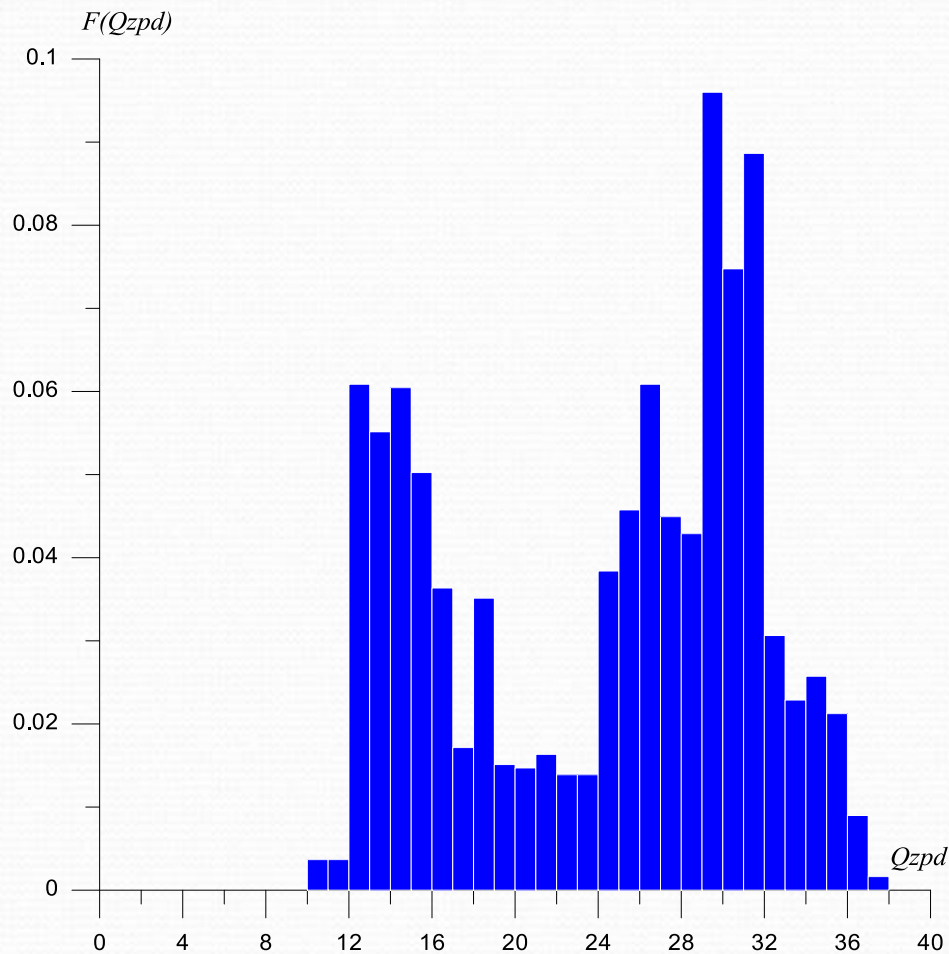


Since the main moisture content in the atmosphere falls on the boundary layer $h = 2.5$ km, the determining condition for choosing the installation points of the MMV antennas is the local climate of a particular territory, which can largely minimize the influence of atmospheric absorption. Therefore, an alternative concept may be to choose a location with a specific wind rose that delivers dry air to the tool installation point. A similar approach was used in the construction of a 64-meter radio telescope on the island. Sardinia (Italy), located at an altitude of only 600 m above sea level and designed to operate up to a wavelength of 3 mm. When choosing the installation site, the arid climate of the island was taken into account.



The roughness of the histograms can be caused by various reasons. The histograms of the integral moisture content in August 2019 for the polygons "Svetloye" (a) and "Badary" (b) are shown. The effect of indentation is associated here with a significant number of cloud situations in these climatic zones of the Russian Federation in August 2019. In this case, the monthly average values of the integral moisture content for these polygons are the only way to adequately describe the existing weather situation. To clarify the average values, large statistics are needed, including several years.

2019 г.



A histogram of the measured values of the integral moisture content in the atmosphere in millimeters of deposited moisture at the Zelenchukskaya landfill with two maxima for August 2019. The histogram is based on 2665 measurements. In this case, a sharp change in the integral moisture content in the middle of the month can be caused both by the passage of a weather front with a drift of dry air, which has a random character, and by the features of the local atmospheric circulation associated with the mountain terrain near the landfill. Further research is needed to answer these questions about the IPA RAS polygons.

1. The results of the study of the integral moisture content obtained from measurements of atmospheric absorption in the wavelength range of 3 mm at the Karadag test site (Republic of Crimea) from August 2019 to January 2020 are presented.
2. A comparative analysis of the MMV propagation conditions is carried out on the basis of the characteristics used in the 80s of the 20th century to select the location of a 70-meter millimeter-wave antenna for the Suffa plateau, the Karadag test site, and three test sites of the IAA RAS.
3. In terms of the number of clear days and nights, Karadag and Suffa are comparable and surpass the ranges of the IAA RAS located in the North Caucasus (Zelenchukskaya), the north of the European part of the Russian Federation (Svetloye) and central Siberia (Badary)
4. A comparative analysis of the values of the integral moisture content that determine the conditions for the propagation of MMV is carried out: for Karadag (August-January 2019-2020 according to measurements of atmospheric absorption in the range of 3 mm), for Suffa (average for 1981-1991 according to aerological data), for three polygons of the IAA RAS (Svetly, Zelenchukskaya and Badara, August-January 2019-2020 according to measurements of tropospheric delay in precision positioning systems).
5. A comparison of the data for Karadag and Suffa shows that one of the main factors associated with the integral moisture content is the surface temperature. At these two sites, at similar temperatures, comparable integral moisture contents are observed. It is shown that the ascent of the antenna to the mountain (the "Suffa" plateau) affects the integral moisture content, but not too significantly, through a decrease in the surface temperature. In the summer-autumn period, the average monthly integral moisture content on Karadag is 5-7 mm higher than for Suffa, which is due to the low summer temperatures on the plateau (altitude 2500 m). In the summer-autumn period, according to this criterion, Karadag is inferior to Suffa, but surpasses the ranges of the IAA RAS. Low integral moisture content for the Suffa and the IPA RAS polygons is observed in winter at subzero temperatures.
6. The consistent application of the principles of comparative analysis used in the selection of the Suffa plateau to the location of the millimeter-wave antennas leads to places with cold climates and long winters with negative temperatures. However, in practice, two concomitant negative factors must be taken into account: 1) the presence in most climatic zones of the Russian Federation of a significant probability of the number of cloud situations; 2) the difficulty of operating precision millimeter-range equipment at sub-zero temperatures, as well as a significant increase in the cost of building tools due to this.
7. The use of monthly average values of the integral moisture content in landfills is too rough a characteristic. In particular, due to the specific wind rose at the Karadag landfill, high air transparency periodically occurs. As a result, even in the summer, the integral moisture content drops to levels comparable to Suffa and other high-altitude telescopes. In this regard, a more detailed daily and intraday distribution of the results of moisture content measurements should be taken into account.

Improving the accuracy of calibration in the millimeter range for measurements of atmospheric radiation by a specialized measuring system.

$$R > \frac{D^2}{\lambda}$$

It is impossible to use the "artificial Moon" method on millimeter waves, because the distance to the far zone of the antenna is too large. In radio astronomy observatories, the modulation calibration method is widely used, which consists in switching the receiver input path from the antenna to a load with a known temperature (the chopper-wheel method). It consists in the fact that before the first amplifier, the so-called chopper is turned on in the path-this is a switch that alternately connects the antenna output and the room-temperature blackbody load to the receiver. Historically, it was used on mm waves due to the lack of corresponding diode noise generators in this range, the signals of which are used for calibrations. The step value of the noise generator signal mixed into the input path is determined by two loads: hot (at room temperature) and cold (liquid nitrogen), and when it is stable, it is then used in the measurement process. The noise generator does not block the input path and atmospheric radiation does not affect the value of the calibration step. But the chopper, which is used on mm instead of a noise generator, blocks the input path and the calibration step is equal to the difference between the signals from the black body and the signal from the atmosphere. In this case, the formula for processing the calibration signal is used without changes. For this reason, as the atmospheric radiation increases, the calibration step decreases and this partially compensates for the increase in the antenna temperature due to the increase in atmospheric radiation. Since the brightness temperature of the atmosphere is not measured, the reasoning is of a qualitative nature. In this case, the atmospheric contribution is part of the calibration error. In [Philip R. Jewell. Millimeter Wave Calibration Techniques. Single-Dish Radio Astronomy: Techniques and Applications, ASP Conference Series, Vol 278, 2002] it is noted that the accuracy of such calibration is 5-10%. Meanwhile, the implementation of two-temperature calibration allows you to separate the noise of the receiver and the atmosphere, measure the parameters of the atmosphere and increase the calibration accuracy to 1%. In this case, the atmospheric parameters are measured by a standard radio astronomy receiver, but the atmosphere is variable, but increasing the number of two-temperature calibrations to follow the changes will significantly complicate the process. The presence of an atmospheric measuring system allows you to determine the parameters of the atmosphere in real time without using two-temperature calibration and increase the accuracy of calibration by an order of magnitude

Specialized radiometric system for atmospheric diagnostics.

$$T_{\mathcal{R}}(\theta) = T_{cp} \left(1 - e^{-\frac{\tau}{\cos\theta}} \right) + 2.73 \cdot e^{-\frac{\tau}{\cos\theta}} \quad Q = \int_0^{\infty} \rho_{H_2O}(h) dh \quad \alpha_{H_2O}(h) = \varphi_{H_2O}(h) \rho_{H_2O}(h) \quad \tau_{H_2O} = \int_0^{\infty} \alpha_{H_2O}(h) dh = \int_0^{\infty} \varphi_{H_2O}(h) \rho_{H_2O}(h) dh \cong \bar{\varphi}_{H_2O}(\lambda) Q$$

$$\tau(\nu_{\alpha}), \alpha = 1, 2 \quad \tau(\nu_{\alpha}) = \tau_{O_2}(\nu_{\alpha}) + \varphi_{H_2O}(\nu_{\alpha}) \cdot Q + \psi_w(\nu_{\alpha}) \cdot W \quad \nu_1 \approx 22.235 \text{ ГГц} \quad \nu_2 \approx 30 \div 40 \text{ ГГц} \quad \nu_3 \approx 56.7 \text{ ГГц}$$

Typically, atmospheric radiation is used in the transparency window at a wavelength of 0.8 cm, the absorption lines of oxygen and water vapor at wavelengths of 0.5 cm and 1.35 cm.

The spectral line H₂O 1.35 cm is weak enough to measure small amounts of water vapor Q in the atmosphere. In this case, it is preferable to use a strong H₂O absorption line 183 GHz (1.64 mm), or rather its long-wave slope in the range of 70-110 GHz, (~3 mm) in the transparency window between the strong atmospheric oxygen absorption lines of 60 GHz and 120 GHz.

$$\tau(\nu_{\alpha}), \alpha = 1, 2 \quad \tau(\nu_{\alpha}) = \tau_{O_2}(\nu_{\alpha}) + \varphi_{H_2O}(\nu_{\alpha}) \cdot Q + \psi_w(\nu_{\alpha}) \cdot W \quad \nu_1 \approx 60 - 90 \text{ ГГц} \quad \nu_2 \approx 30 \div 40 \text{ ГГц} \quad \nu_3 \approx 56.7 \text{ ГГц}$$

The sensitivity to changes in the water vapor content Q in the 1.64 mm line, for example, at a frequency of 140 GHz, is 3.5 times greater than in the traditional range of the H₂O study in the 1.35 cm line.

$$\text{Absorption at the radio telescope frequency } \tau(\nu_{pm}) \quad \tau(\nu_{pm}) = \tau_{O_2}(\nu_{pm}) + \varphi_{H_2O}(\nu_{pm}) \cdot Q + \psi_w(\nu_{pm}) \cdot W$$

$$\text{Tropospheric delay the signal } \lambda \geq 1 \text{ mm} \quad \Delta l_{\varphi} [cm] = \int_0^{H_A} (n - 1) dl = \sec\theta \left(0.2279 \cdot P_0 [zPa] + 0.109 \cdot Q [z/cm^2] + \frac{1730}{T_Q [K]} Q [z/cm^2] + 0.145 \cdot W [kg/m^2] \right)$$

The millimeter range complex will have:

Higher accuracy of measurement of atmospheric parameters;

High spatial resolution;

Lower weight and overall characteristics;

High noise immunity; It will be adaptive, which will allow you to measure the absorption at both medium and low moisture contents;

The ability to measure the tropospheric signal delay for VLBI and GLONASS at both medium and low moisture content.

Measure the parameters of the atmosphere in the desired direction by the brightness temperature for small periods of time (if there is an absolute calibration).

$\nu_1 \approx 22.235 \text{ ГГц}$

$\nu_3 \approx 56.7 \text{ ГГц}$

Обычно используется излучение атмосферы в окне прозрачности на длине волны 0.8 см, линиях поглощения кислорода и водяного пара на длинах волн 0.5 см и 1.35 см.

Ильин Г.Н., Троицкий А.В. // Известия высших учебных заведений. Радиофизика. 2017. Т. 60. № 4. С. 326.
 Караваев Д.М. СВЧ-радиометрические исследования влагозапаса атмосферы и водозапаса облаков // Автореферат диссертации на соискание уч. степ. канд. техн. наук, Санкт-Петербург, 2010.
 В.Д. Степаненко, Г.Г. Шукин, Л.П. Бобылев, С.Ю. Матросов «Радиотеплолокация в метеорологии», Л., Гидрометеоиздат, 1987

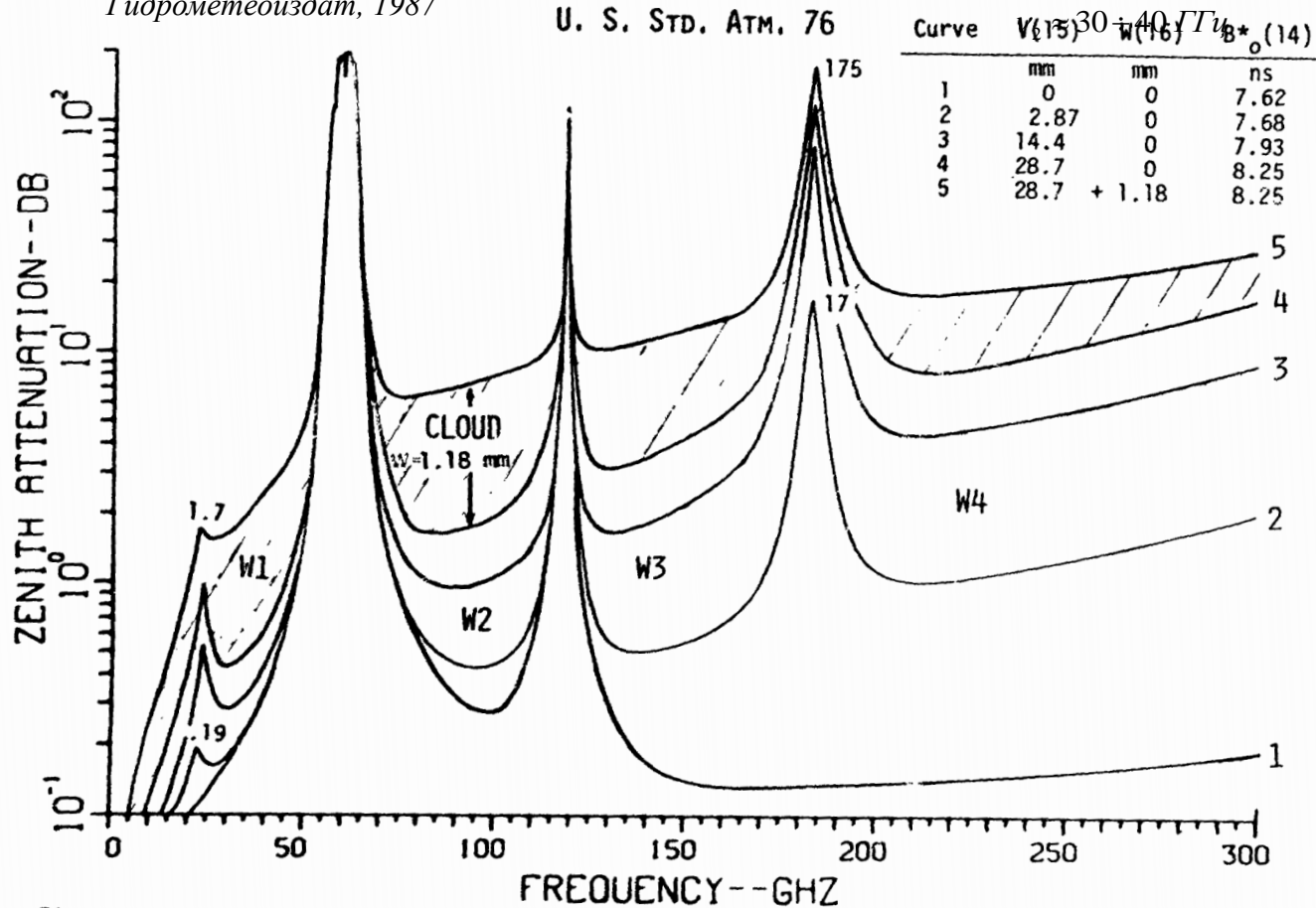


Figure 9. One-way Zenith attenuation A_z over a frequency range from 5 to 300 GHz (resolution 2.5 GHz) through the U.S. Standard Atmosphere (NOAA, 1976) assuming dry and moist air masses including a rain-bearing cloud calculated with Program P1. The symbols W1 to W4 indicate the millimeter wave window ranges.

$\nu_1 \approx 60 - 90 \text{ ГГц}$

$\nu_2 \approx 30 \div 40 \text{ ГГц}$

$\nu_3 \approx 56.7 \text{ ГГц}$

Спектральная линия H_2O $\lambda = 1,35 \text{ см}$ является достаточно слабой для измерения малых содержаний водяного пара Q в атмосфере. В этом случае предпочтительно использовать сильную линию поглощения H_2O $\nu = 183 \text{ ГГц}$ ($\lambda = 1,64 \text{ мм}$), а точнее ее длинноволновый склон в диапазоне 70-110 ГГц.

Obtaining atmospheric radiation absorption for a number of angles from 0 to 80 degrees from the zenith, and a reference region with a brightness temperature close to the surface air temperature.



2019 г.

Taking into account the experience of measurements in 2017 and 2018, a new radiometric complex (RC) was created, including radiometers at wavelengths of 3 mm and 8 mm, as well as a professional weather station Davis Vantage Pro 2. With the help of the RC, atmospheric absorption measurements were carried out at the Karadag test site from August 2019 to January 2020. To ensure the autonomous round-the-clock operation of the complex in a wide range of temperatures, a new robust housing with a thermal stabilization system and a data transmission system via the Internet was created. In the above-mentioned time interval of 2019-2020, measurements were carried out only by one 3 mm channel of the radiometer, the receiver of the 8 mm channel passed the testing mode. The complex uses a modulation radiometer with an operating frequency band from 92.5 GHz to 96.4 GHz.

All algorithms for processing data obtained by the method of atmospheric sections are based on the use of dimensionless ratios of signal increments at the output of the radiometric receiver.

$$T_{Я}(\theta) = T_{cp} \left(1 - e^{-\frac{\tau}{\cos \theta}} \right) + 2.73 \cdot e^{-\frac{\tau}{\cos \theta}} \quad d(\theta) = k \cdot T_{Я}(\theta) + A \quad Y(\tau) = \frac{d(\theta_2) - d(\theta_1)}{d(\theta_3) - d(\theta_2)} = \frac{T_{Я}(\theta_2) - T_{Я}(\theta_1)}{T_{Я}(\theta_3) - T_{Я}(\theta_2)} = \frac{\exp\left(-\frac{\tau}{\cos \theta_2}\right) - \exp\left(-\frac{\tau}{\cos \theta_1}\right)}{\exp\left(-\frac{\tau}{\cos \theta_3}\right) - \exp\left(-\frac{\tau}{\cos \theta_2}\right)}$$

$$T_{cp} - T_{Я}(\theta) = T_{cp} \cdot e^{-\frac{\tau}{\cos \theta}} \quad \ln(d_0 - d(\theta)) = -\frac{\tau}{\cos \theta} + \ln(kT_{cp})$$

The ratio in τ is linear, which makes it possible to use the least squares method to determine it and obtain statistically justified parameter errors. Another advantage of this modification of this method is that any number of angles in the range from the zenith can be used to improve the measurement accuracy. The measurement error given by the least squares method was used as an indicator of the occurrence of individual clouds in the antenna radiation pattern at certain angles. This is due to the fact that, despite the selection of weather situations with clouds of less than 2.5 points, the clouds could fall into the antenna radiation pattern at certain angles. The criterion introduced in this way made it possible to exclude from consideration measurements in which the resulting error exceeded 1% of the average absorption value.

Combined measurement method

Section method + Atmospheric calibration + Measurement of atmospheric absorption in the desired direction with the radiometer time constant

$$T_{\mathcal{R}}(\theta, t, \lambda) = T_A(\theta = 0^\circ, t, \lambda) + 2.73 \cdot e^{-\tau}$$

$$T_A(\theta) = T_{cp} \left(1 - e^{-\tau \cdot \sec \theta} \right)$$

$$T_{cp} = \frac{T_0 - 2.73 \cdot \left[e^{-\tau \sec \theta_2} \frac{n(d_0) - n(\theta_1)}{n(\theta_2) - n(\theta_1)} - e^{-\tau \sec \theta_1} \frac{n(d_0) - n(\theta_2)}{n(\theta_2) - n(\theta_1)} \right]}{1 - \left[e^{-\tau \sec \theta_2} \frac{n(d_0) - n(\theta_1)}{n(\theta_2) - n(\theta_1)} - e^{-\tau \sec \theta_1} \frac{n(d_0) - n(\theta_2)}{n(\theta_2) - n(\theta_1)} \right]}$$

$$T_{cp}(\lambda) = \frac{\int_0^{\tau \sec \theta} T(h_A) e^{-\tau' \sec \theta} d\tau' \sec \theta}{\int_0^{\tau \sec \theta} e^{-\tau' \sec \theta} d\tau' \sec \theta}$$

it makes sense for the temperature of a uniformly heated atmosphere to produce the same radiation in a given direction as an atmosphere with a valid temperature distribution over altitude

measurement of the optical thickness of the atmosphere in the transparency windows of 3 and 8 mm



Diagnostics of atmospheric parameters in the short-wave part of the millimeter range

$$d(\theta) = k \cdot T_{\mathcal{R}}(\theta) + A$$

adaptive $\tau \sim 1$

$$T_{\mathcal{R}}(\theta, t, \lambda) = T_A(\theta, t, \lambda) + 2.73 \cdot e^{-\tau}$$

$$\tau(\nu_\alpha), \alpha = 1, 2$$

$$\tau(\nu_\alpha) = \tau_{O_2}(\nu_\alpha) + \varphi_{H_2O}(\nu_\alpha) \cdot Q + \psi_w(\nu_\alpha) \cdot W$$

$$\nu_1 \approx 60 - 90 \text{ ГГц}$$

$$\nu_2 \approx 30 - 40 \text{ ГГц}$$

$$\nu_3 \approx 56.7 \text{ ГГц}$$

$$\Delta l_\phi [cm] = \int_0^{H_A} (n - 1) dl = \sec \theta \left(0.2279 \cdot P_0 [zPa] + 0.109 \cdot Q [z/cm^2] + \frac{1730}{T_Q [K]} Q [z/cm^2] + 0.145 \cdot W [kg/m^2] \right)$$

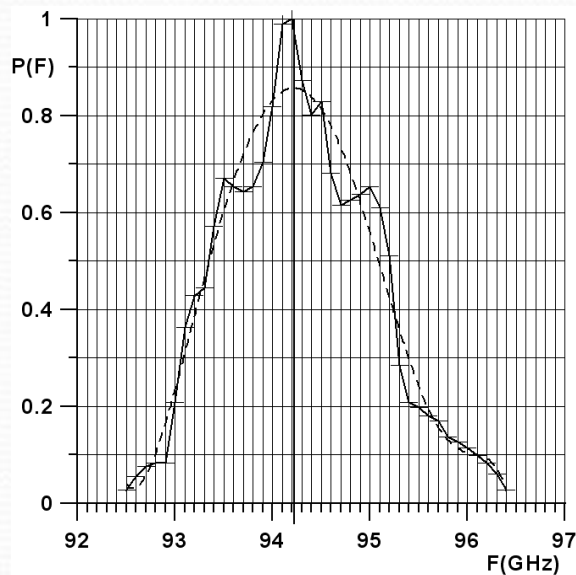


2018 г.



Image of the assembly and preliminary testing of the 3mm channel of the radiometer

A two-channel version of the radiometer assembly on the roof of the hardware house of the Karadag test site during calibration.

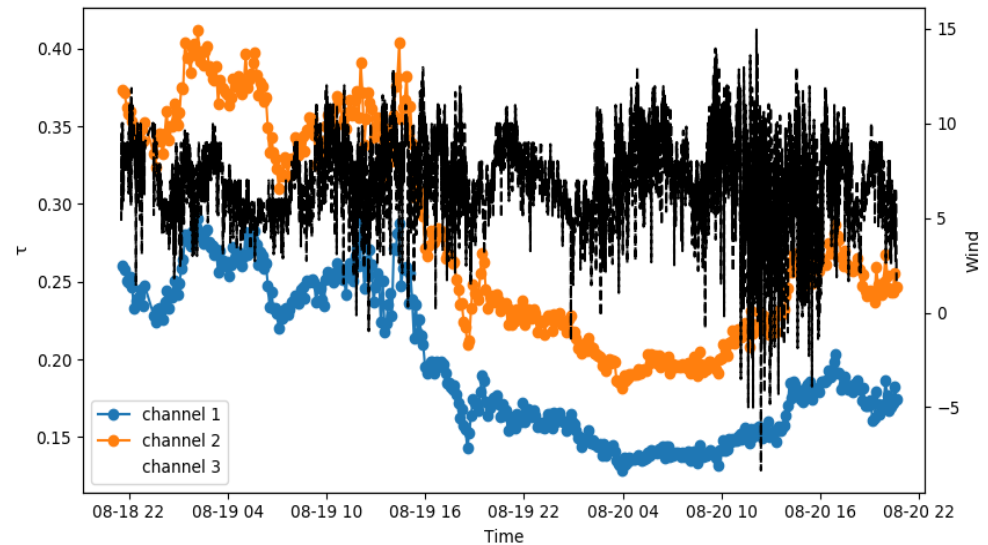
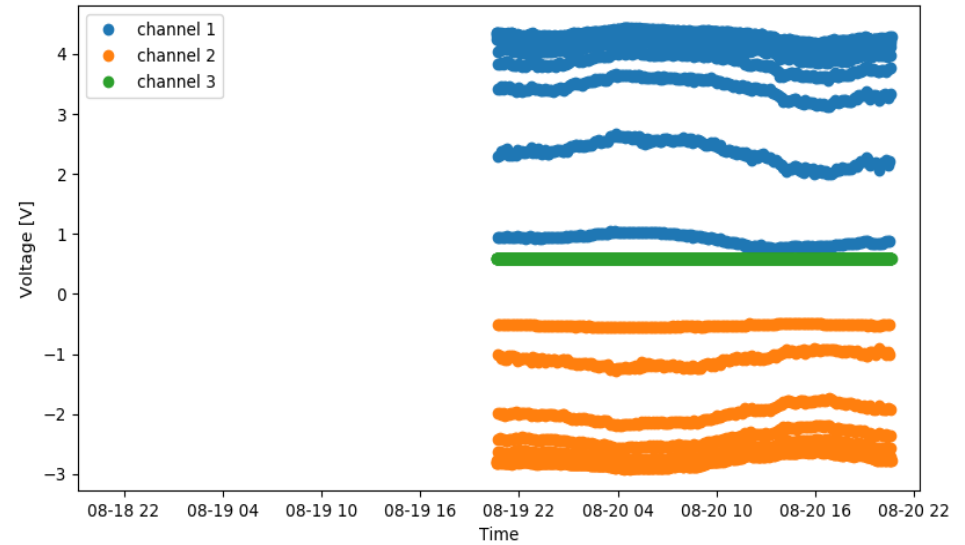


The amplitude-frequency response of the 3 mm channel of the radiometer.



Measurement of atmospheric absorption at Karadag

Measurement of atmospheric absorption at the Karadag test site (data recording, processing and transmission system)



В настоящее время для получения интегральной влажности и водности атмосферы, профиля температуры используются радиометрические системы работающие в коротковолновой части сантиметрового диапазона



MTP-5

Метеорологический температурный профилемер (Россия)

<http://www.raimet.ru/equipment/temperature-profilers/213/>

Традиционно, для дистанционного определения влаго- и водозапаса, температурного зондирования и тропосферной задержки радиосигнала используется излучение атмосферы в окне прозрачности на длине волны 0.8 см, линиях поглощения кислорода и водяного пара на длинах волн 0.5 см и 1.35 см. Такие системы в настоящее время предлагается использовать для коррекции тропосферной задержки радиосигнала в спутниковых навигационных системах и радиоастрономии, для дистанционного зондирования атмосферы и прогноза опасных гидрометеорологических явлений .



**Температурный профилемер (радиометр)
RPG-HATPRO (Германия)**

<http://www.raimet.ru/equipment/temperature-profilers/255/#>



Радиометр водяного пара ИПА РАН

<http://iaaras.ru/quasar/wvr/>